Formation of luminescent Si nanocrystals by high-temperature rapid thermal chemical vapor deposition

Hea Jeong Cheong, Jung Hyun Kang, Jae Kwon Kim, Yong Kim,[a] Jae-Yel Yi, Tae Hun Chung, and Hong Jun Bark
Department of Physics, Dong-A University, Hadan-2-dong, Sahagu, Pusan 604-714, Korea

(Received 16 June 2003; accepted 18 August 2003)

We observe a completely different growth regime of silicon-rich oxide (SRO) layers by rapid thermal chemical vapor deposition for the formation of luminescent nanocrystals. The growth regime is characterized by low $[N_2O]/[SiH_4]$ ratios (<1) and high growth temperatures ($>700\,^{\circ}C$). High-resolution cross-sectional transmission electron microscopy (XTEM) shows the bimodal distribution of large polycrystals and nanocrystals after post-deposition annealing. The luminescence is attributed to the nanocrystals. Fourier transform infrared spectroscopy in conjunction with XTEM and energy-dispersive x-ray studies show the phase separation and bonding reconfiguration in as-deposited SRO layers. The effectively increased oxygen content in the oxide matrix by phase separation and bonding reconfiguration reduces the diffusion coefficient of Si in the matrix, resulting in the formation of nanocrystals during post-deposition annealing. © *2003 American Institute of Physics.* [DOI: 10.1063/1.1616646]

Since the first discovery of light emission from porous silicon,[1] interest in Si-based optoelectronics has rapidly increased. Due to the better compatibility with standard ultra-large-scale integrated (ULSI) circuit processes, Si nanocrystals in a dielectric matrix have gained much interest. The standard approach for the formation of Si nanocrystals is the utilization of the prolonged annealing of substoichiometric silicon oxide at temperatures higher than 900 °C. During the annealing, phase separation and precipitation take place owing to the energetic stability of Si and SiO_2 phases. The methods for the formation of substoichiometric silicon oxide include ion implantation,[2] plasma-enhanced chemical vapor deposition (PECVD),[3] low-pressure CVD (LPCVD),[4–6] reactive evaporation,[7] cosputtering,[8] pulsed laser deposition,[9] etc. Silicon-rich oxide (SRO) layers containing ~50 at % O yield highly luminescent nanocrystals with large density regardless of growth methods. Furthermore, growth temperatures for the SRO layers were usually below 650 °C for maintaining an amorphous phase in as-deposited SRO layers.

The rapid thermal chemical vapor deposition (RTCVD) apparatus has been emerged as the next-generation cluster tool for ULSI technology.[10] The growth by RTCVD proceeds via limited reaction processing.[11] Thus, the inherently RTCVD apparatus is a single-wafer-based processing tool, thereby requiring a high growth rate of more than 100 nm/min for competitive throughput, as compared to LPCVD.[10] Despite the importance of the RTCVD method, little work has been done specifically on the growth of SRO layer, except for a report aiming at the growth of stoichiometric SiO_2.[12]

SRO layers were grown by a home-built RTCVD. Processing gases were 20% Ar-diluted SiH_4 and N_2O. A bank of tungsten-halogen lamps allows the rapid heating of a 3 in. Si wafer with the ramp rate of 80 °C/min. Wafer temperatures, calibrated by a thermocouple, were monitored by an infrared pyrometer (IRCON with a 5 μm detection band) through a sapphire window. Si wafers were inverted and supported by quartz pins, and source gases were injected from the bottom of a cold-wall reaction chamber. Such an inverted structure ensures the minimal inclusion of particulates. The chamber pressure was maintained by a feedback operation of a MKS throttle valve and a Baratron gauge. The chamber pressure was kept at 3 Torr throughout the present experiment. The flow rate of SiH_4 was 16 sccm and the flow rate of N_2O was a variable parameter. The growth temperature T_g was varied from 650 to 800 °C. SRO layers were subsequently annealed at 1100 °C for 2 h in N_2 ambient. Some samples were further annealed at 450 °C for 1 h in a forming gas (N_2 95%, H_2 5%) to investigate the H_2 passivation effect. Photoluminescence (PL) spectra were excited by a 488 nm Ar^+ ion laser (30 mW and ~1 mm beam diameter). PL emissions were dispersed by a 0.5 m monochrometer (Dongwoo Optron DM500). The PL signal was detected by a photomultiplier tube (Hamamatsu R928). The observed PL spectra were corrected using a tungsten-halogen lamp. The cross-sectional transmission electron microscope (XTEM) was observed by using a JEOL JEM-2010 through a standard preparation technique. The oxygen and silicon contents in the layer were analyzed by energy-dispersive x-ray (EDX) measurements (OXFORD INCA) attached to the TEM equipment. The bonding configurations in oxide matrix were measured by a Fourier transform infrared spectroscope (FTIR, Biorad Excalibur FTS-3000).

First, we grow several SRO layers with various $[N_2O]/[SiH_4]$ ratios at 650 °C. The growth rate decreases as the $[N_2O]/[SiH_4]$ ratio increases. This is due to the decrease of the partial pressure of SiH_4 since the total pressure is kept at 3 Torr. After post-deposition annealing, we observe very weak PL emission for samples with $1<[N_2O]/[SiH_4]<5$. The size of Si crystallites critically depends on [O] in the layer and exceeds the size of the nanocrystal for quantum confinement effect for the layers with low $[N_2O]/[SiH_4]$ ra-

[a]Electronic mail: yongkim@daunet.donga.ac.kr

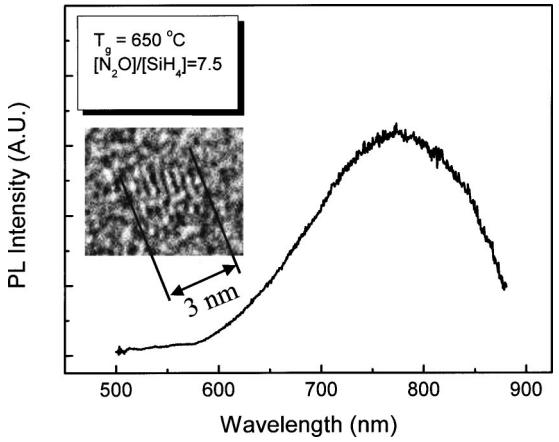

FIG. 1. PL spectra of the SRO layer deposited with $[N_2O]/[SiH_4]=7.5$ and $T_g=650$ °C after post-deposition annealing. The inset shows the XTEM image of a typical nanocrystal.

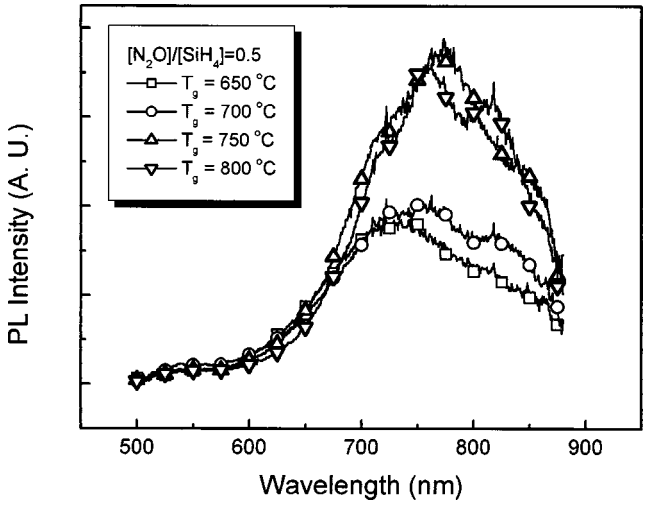

FIG. 2. PL spectra of SRO layers grown at various growth temperatures with $[N_2O]/[SiH_4]=0.5$ after the high-temperature N_2 annealing and additional forming gas annealing.

tios. For the samples with $[N_2O]/[SiH_4]>5$, SRO layers start to emit PL after annealing. Specifically, for samples with $[N_2O]/[SiH_4]=7\sim8$, we observe the most intense PL emission. Figure 1 shows the PL spectra for the sample with $[N_2O]/[SiH_4]=7.5$ after post-deposition annealing. The center wavelength is at 770 nm. The inset shows the XTEM image of a typical nanocrystal ($\sim$3 nm diameter) found in the sample. The observed [O] in the layer by EDX is $\sim$53 at. %. Therefore, the result is in good agreement with reports by Lombardo *et al.*[4,5] Lombardo *et al.*[5] have reported intense PL emissions from SRO layers with the range of [O] between 52 and $\sim$58 at. % grown by LPCVD at 625 °C. However, the growth rate for $[N_2O]/[SiH_4]=7.5$ is only $\sim$10 nm/min, far below the required growth rate for RTCVD,[10] although acceptable for batch-process-based LPCVD. The thickness of the SRO layer in Fig. 1 is about 600 nm, and the growth was done by several heating/cooling procedures to avoid overheating of RTCVD chamber. The cumulative growth time was 1 h. One practical way to obtain an applicable growth rate is to increase growth temperature. Since the growth by RTCVD is in the surface-controlled regime, the growth rate increases exponentially as a function of the growth temperature.[13]

Figure 2 shows the PL spectra of the annealed SRO layers (N_2 annealing + forming gas annealing) with $[N_2O]/[SiH_4]=0.5$, but having various growth temperatures. The luminescence is scaled to the thickness for reasonable comparison. The PL intensities increase with increasing growth temperatures. The SRO layer with $T_g=750$ °C shows the largest PL intensity, and the intensity is about 30% of the sample with the equivalent thickness, but with $[N_2O]/[SiH_4]=7.5$. It is noteworthy that the growth rate for SRO layers with $T_g\geqslant700$ °C is more than 200 nm/min. Thus, the growth rates meet the requirement for the practical application of RTCVD.

The finding in Fig. 2 is contrary to the generally accepted idea that increasing the growth temperature results in the growth of too-large crystallites to give any quantum confinement effect. To clarify the origin of the luminescence, we investigate the XTEM of the SRO layers. Figure 3(a) shows the XTEM image of the as-deposited SRO layer with $T_g=750$ °C. The layer contains a large density of polycrystals, as expected. The transmission electron diffraction (TED) pattern shown in the inset further confirms the existence of the large polycrystals. Besides diffraction rings, many spots representing polycrystalline states are visible. Figure 3(b) shows the XTEM image of the annealed SRO layer. Very large polycrystals are observed. The TED pattern shows more distinct spots with sharper diffraction rings compared to that of the as-deposited sample. This confirms the further growth of polycrystals during the annealing. Interestingly, we observe many nanocrystals together with very large polycrystals [see Fig. 3(b)]. Therefore, the XTEM result may give a clue that the luminescence we observe originated from the nanocrystals. The PL intensities, as shown in Fig. 2, are enhanced by a factor of approximately 2 compared to those without forming gas annealing. If the PL originates from the

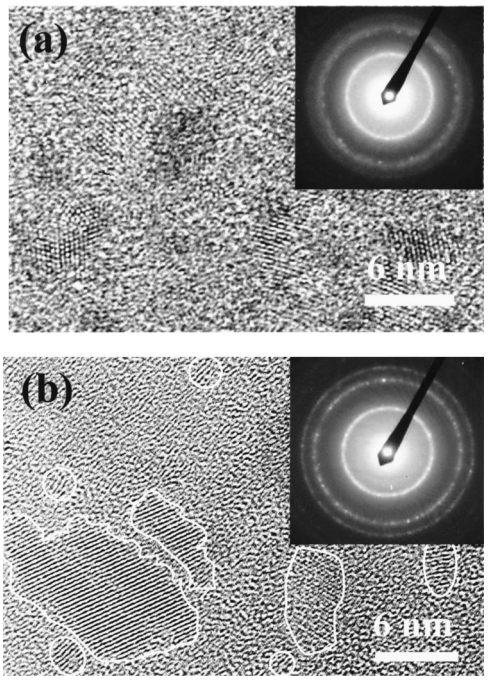

FIG. 3. XTEM images of SRO layer with $[N_2O]/[SiH_4]=0.5$ and $T_g=750$ °C before (a) and after (b) annealing. The insets show the TED patterns. White boundaries in (b) is for a guide to an eye.

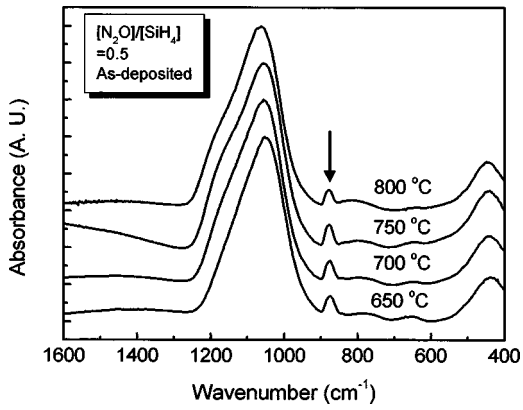

FIG. 4. Infrared spectra of as-deposited SRO layers with various growth temperatures. The spectra are shifted for clarity. Note the appearance of the peaks at 880 cm^{-1} (marked by an arrow) regardless of the growth temperature.

radiative recombination related to some specific defects, the forming gas annealing would quench the PL.[14]

Figure 4 shows the FTIR spectra for as-deposited SRO layers with various growth temperatures. The IR band around 1050~1080 is attributed to a Si–O–Si asymmetric stretching mode vibration. For the SRO layer with T_g=650 °C, a Si–O–Si stretching mode band is observed at 1050 cm^{-1}. According to Pai *et al.*,[15] the Si–O–Si stretching mode shifts linearly with the oxygen content, provided that the layer is homogeneous. The systematic shift of the Si–O–Si stretching mode band due to the increase of oxygen content is observed as increasing the growth temperature. In addition, the broad band of the Si–O–Si asymmetric stretching band develops into the peak with a shoulder due to the separation of in-phase and out-of-phase vibrations.[16] This is another indication of the increase of the oxygen content in the oxide matrix. The scattered data[15,17,18] of the Si–O–Si asymmetric stretching mode variation with oxygen content give an difficulty in determining the at. % of [O] in the matrix. Adopting the parameterized equation by Zacharias *et al.*,[17] the estimated [O] in Fig. 4 is 50 at. % at 650 °C and 54 at. % at 750 °C. However, [O] for SRO layers at 650 and 750 °C, determined by EDX, are only 19 and 24 at. %, respectively. The strong discrepancy between FTIR and EDX results indicates that the layers are no longer homogeneous, and significant phase separation and bonding reconfiguration occur even for the sample at 650 °C. In addition, an IR band at 880 cm^{-1} is repeatedly observed regardless of the growth temperature. The band was previously ascribed to the stretching vibration of the Si–N bond by Iacona *et al.*[3] for PECVD samples with SiH_4/N_2O chemistry. However, Yi *et al.*[19] reported the appearance of IR bands at 880 cm^{-1} after annealing at a temperature range of 300 to 600 °C for samples grown by reactive evaporation (i.e., nitrogen-free environment). The IR band gradually disappeared at the elevated annealing temperatures. We observe a similar disappearance of the IR band after the annealing at 1100 °C accompanied with the spectral shift of the Si–O–Si stretching mode to 1080 cm^{-1}. The position of 1080 cm^{-1} corresponds to the characteristic Si–O–Si stretching mode vibration of pure SiO_2. Yi *et al.* have ascribed the band at 880 cm^{-1} to Si ring configurations isolated by oxide.[19] The Si rings have a role of the basic cells for future Si nanocrystals.

For SRO layers with low $[N_2O]/[SiH_4]$ (i.e., <1), high T_g ($T_g \geqslant 700$ °C), effective oxygen content in the oxide matrix is much higher than average oxygen content due to phase separation and bonding reconfiguration. Furthermore, the oxide matrix contains a large density of Si ring structures, which could be transformed to nanocrystals during subsequent annealing. During post-deposition annealing, preexisting polycrystals grow further. Nanocrystals, presumably responsible for the luminescence, are generated from Si rings. Hence, this is an extreme example of a bimodal distribution (i.e., very large polycrystals and nanocrystals). The nanocrystal growth rate depends linearly on the diffusion coefficient of Si.[20] The diffusion coefficient is extremely sensitive to the oxygen content in the oxide matrix.[4] For instance, Lombardo *et al.*[4] have reported two orders of magnitude difference of diffusion coefficients of Si in SRO layers with 10 and 27 at. % O. Phase separation and bonding reconfiguration effectively increase the oxygen content in the oxide matrix. In this case, the reduced diffusion coefficient of Si in the matrix yields nanocrystals with an appreciable quantum confinement effect after post-deposition annealing.

The work is supported by the research program from Electronics and Telecommunications Research Institute (ETRI), as a part of project entitled ''Development of technology toward nanodevices with high functionality for information and communication.''

[1] L. T. Canham, Appl. Phys. Lett. **57**, 1046 (1990).
[2] K. S. Min, Ph.D. thesis, Caltech, 2000.
[3] F. Iacona, G. Franzo, and C. Spinella, J. Appl. Phys. **87**, 1295 (2000).
[4] S. Lombardo and S. U. Campisano, Mater. Sci. Eng., R. **17**, 281 (1996).
[5] S. Lombardo, S. Coffa, C. Bongiorno, C. Spinella, E. Castagna, A. Sciuto, C. Gerardi, F. Ferrari, B. Fazio, and S. Privitera, Mater. Sci. Eng., B **69–70**, 295 (2000).
[6] P. Bruesch, Th. Stockmeier, F. Stucki, and P. A. Buffat, J. Appl. Phys. **73**, 7677 (1993).
[7] M. Zacharias, J. Heitmann, R. Scholz, U. Kahler, M. Schmidt, and J. Blasing, Appl. Phys. Lett. **80**, 661 (2002).
[8] M. Fujii, S. Hayashi, and K. Yamamoto, Jpn. J. Appl. Phys. **30**, 687 (1991).
[9] L. Patrone, D. Nelson, V. I. Safarov, M. Sentis, W. Marine, and S. Giorgio, J. Appl. Phys. **87**, 3829 (2000).
[10] C. Y. Chang and S. M. Sze, *ULSI Technology* (McGraw-Hill, New York, 1996), Chap. 4.
[11] J. F. Gibbons, C. M. Gronet, and K. E. Williams, Appl. Phys. Lett. **47**, 721 (1986).
[12] X. L. Xu, R. T. Kuehn, J. J. Wortman, and M. C. Ozturk, Appl. Phys. Lett. **60**, 3063 (1992).
[13] X. Ren, M. C. Ozturk, J. J. Wortman, B. Zhang, D. M. Maher, and D. Batchelor, J. Vac. Sci. Technol. B **10**, 1081 (1992).
[14] K. S. Min, K. V. Shcheglov, C. M. Yang, H. Atwater, M. L. Brongersma, and A. Polman, Appl. Phys. Lett. **69**, 2033 (1996).
[15] P. G. Pai, S. S. Chao, Y. Takagi, and G. Lucovsky, J. Vac. Sci. Technol. A **4**, 689 (1986).
[16] G. Lucovsky, M. J. Manitini, J. K. Srivastava, and E. A. Irene, J. Vac. Sci. Technol. B **5**, 530 (1987).
[17] M. Zacharias, D. Dimova-Malinovka, and M. Stutzmann, Philos. Mag. B **73**, 799 (1996).
[18] P. Bruesch, Th. Stockmeier, F. Stucki, P. A. Buffat, and J. K. N. Linder, J. Appl. Phys. **73**, 7690 (1993).
[19] L. X. Yi, J. Heitmann, R. Scholz, and M. Zacharias, Appl. Phys. Lett. **81**, 4248 (2002).
[20] L. A. Nesbit, Appl. Phys. Lett. **48**, 38 (1985).